Building and Environment 112 (2017) 250–260

Contents lists available at ScienceDirect

Building and Environment

journal homepage: www.elsevier.com/locate/buildenv

Simple and accurate temperature correction for moisture pin calibrations in oriented strand board

C.R. Boardman*, Samuel V. Glass, Patricia K. Lebow

Forest Products Laboratory, USA

ARTICLE INFO

Article history:
Received 29 September 2016
Received in revised form
21 November 2016
Accepted 22 November 2016
Available online 24 November 2016

Keywords:
Moisture pin
Oriented strand board
Moisture content
Resistance
Calibration
Temperature

ABSTRACT

Oriented strand board (OSB) is commonly used in the residential construction market in North America and its moisture-related durability is a critical consideration for building envelope design. Measurement of OSB moisture content (MC), a key determinant of durability, is often done using moisture pins and relies on a correlation between MC and the electrical resistance (R) of the OSB between the pins. Early work on these correlations focused on solid lumber and recent correlations for engineered wood products lack data regarding the temperature effects on R. We provide data on 1001 resistance measurements in OSB, sourced from three different locations, over a wide temperature (−17 °C–70 °C) and relative humidity (35%–95%) range. This data, in conjunction with gravimetric MC readings, is used to test existing correlations and support a new simple, accurate formula for calculating MC from resistance and temperature measurements in OSB.

1. Introduction

Oriented strand board (OSB) structural panel sheathing has been used in the North American residential construction market for several decades (see Zerbe [1] for a history of development). OSB has moisture transfer properties that differ from both plywood and construction lumber [2,3]. Moisture-related durability is a critical consideration in building envelope design, particularly when insulation levels and airtightness of wall and roof assemblies are increased or new materials are introduced. Over the last 15 years a large number of field studies in various North American climates have monitored the hygrothermal performance of wall and roof assemblies that include OSB sheathing [4–24]. The moisture content (MC) of OSB sheathing is a key criterion for evaluation of field moisture performance. Moisture accumulation in wood-based materials can lead to mold growth, fungal decay, corrosion of embedded metal fasteners, expansion-contraction damage, and loss of structural capacity. Development of mathematical models for some of these damage functions is the subject of ongoing research [25–35]. While mold growth depends on surface water activity (rather than bulk moisture content, though these are related), the other types of damage are dependent on moisture content. For example a common rule of thumb suggests keeping wood products below 20% MC to minimize risk of decay [36–38]. In addition, questions about moisture risk have driven the ongoing interest in validation and tuning of hygrothermal models as well as parametric analysis [39–48] which allow the prediction of OSB moisture performance during the design of building envelope assemblies. Verification of the models depends on accurate measurement of MC in field and laboratory studies to compare to model prediction.

A common method for measuring moisture content of wood products in the field is through use of a moisture meter, which allows immediate spot readings, or installation of moisture pins with a data acquisition system for long term monitoring. Other researchers rely on direct gravimetric measurement which requires obtaining the mass of a wood sample before and after oven drying. Direct measurement, however, can be cumbersome in practice when applied to field experiments as it relies on either cutting out a specimen or inserting and removing a wood plug from a location in the assembly that may not be readily accessible [49]. While highly accurate, the method is labor intensive and may limit the frequency and extent of data collection. But it does find use in laboratory studies such as [50] which also illustrates the use of OSB outside the North American context as an interior vapor retarder. So while direct gravimetric measurement has its place, and OSB can be used

* Corresponding author. Forest Products Laboratory, U.S. Forest Service, 1 Gifford Pinchot Dr., Madison, WI 53726, USA.
E-mail address: cboardman@fs.fed.us (C.R. Boardman).

http://dx.doi.org/10.1016/j.buildenv.2016.11.039
0360-1323/Published by Elsevier Ltd.

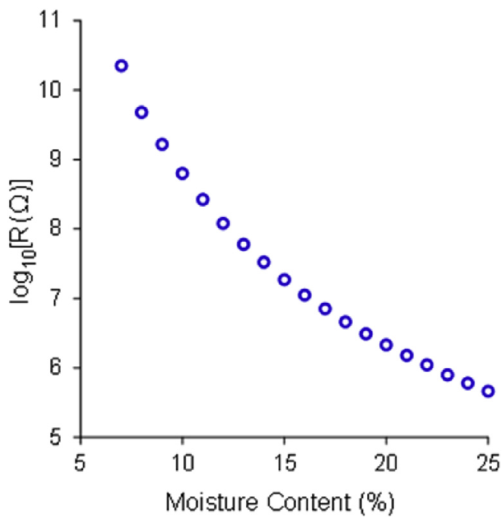

Fig. 1. Resistance vs moisture content in Douglas-fir at 27 °C (80 °F).

for applications besides exterior sheathing, our work seeks to improve the practice of using moisture pins to measure MC in OSB commonly used as exterior sheathing where the risk of moisture accumulation is elevated (relative to interior use). A number of excellent guides to these field measurements are available [51,52]. These systems measure the resistance (R) between the two pins fastened into the wood and assume a correlation between the resistance and the MC. That correlation, and the variability of wood itself, makes this method inherently less accurate than a direct gravimetric measurement of the MC. Early work by William James identified the many factors that influence moisture meter readout [53], and he presented a table with resistance at various MC points for a variety of wood species [54]. That basic correlation for Douglas-fir, which is shown in Fig. 1, provided the foundation for much current work and many commercial moisture meters.
The correlation for Douglas-fir at 27 °C (80 °F) can be expressed[1] as:

$$\log_{10}(MC) = 2.971 - 2.086\,\log_{10}[\log_{10}(R)] \tag{1}$$

This correlation, like much of the work on moisture meters, is valid near room temperature. When moisture meter users want to find MC at different temperatures a correction is applied, which is often based on the extensive work of Pfaff and Garrahan extending the original work by James [55–57]. Their correction factors for species and temperature include a large number of wood species but did not cover engineered wood like OSB. Dissatisfaction with the complicated form of the Garrahan temperature correction, along with the two step nature of the calculation, was a significant motivation for undertaking our study. We want a simple and direct correlation that always includes temperature. There has not been enough attention paid to the temperature effects on moisture meters and very little published data exists supporting the temperature correction factors in engineered wood products. For example, moisture meter correction factors for untreated and ACQ treated plywood were provided by Boardman et al. [58] but did not include temperature compensation. Correction factors for OSB by Carll et al. [5] and Maref et al. [59] similarly were developed only at room temperature.

[1] This fit minimizes the error in prediction for MC based on James' data [54] and differs slightly from the fit provided by Straube et al. [52] which apparently minimized the error in $\log_{10}$(MC).

The lack of temperature correction factors for moisture content of engineered wood products introduces an unquantified measurement uncertainty in field investigation of new assemblies. Temperature correction can be particularly important for wall sheathing in cold climates and roof sheathing in any climate. The observation that the electrical conductivity of wood increases with increasing temperature has been known for over 50 years [53]. Further this suggests "that in wood the mechanism of conduction is by charge carriers whose number or mobility is increased by thermal activity" [53]. Recent work by Zelinka et al. [60] advanced understanding of electrical conductance of wood though a percolation model that explains conductivity due to water pathways when the MC is 16% or more. Below the percolation threshold the conduction mechanisms are still not clear, and empirical models that reflect diffusion theory and Arrhenius equations provide some guidance on how the conductance responds to temperature (pg. 175 Hummel [61], see also [62,63]). Given this background, further work on temperature correction is warranted, especially for engineered wood products.

The present study is part of a larger effort to understand the effects of external insulation on OSB drying in a variety of test walls. To get accurate measurement of the MC of the OSB we compiled a number of OSB moisture pin correlations recently in use, including the method used by the moisture pin equipment manufacturer. Fig. 2 presents these OSB correlations at room temperature, along with James' Douglas-fir data for reference [54]. Although the correlations all indicate that OSB is more conductive than Douglas-fir lumber, they differ considerably when used to predict OSB moisture content. For example, a resistance reading of 1 MΩ (10^6 Ω) would yield an OSB moisture content of about 17% using one correlation but about 21% using another correlation. The reasons for this large variation are not clear. The form of the correlation may not reflect well the underlying physics, or the fit may have been taken on too few samples, or the samples themselves may have differed because of different OSB manufacturing techniques and wood species used. We set out to improve on these existing correlations while also establishing a better understanding of how OSB sourced from

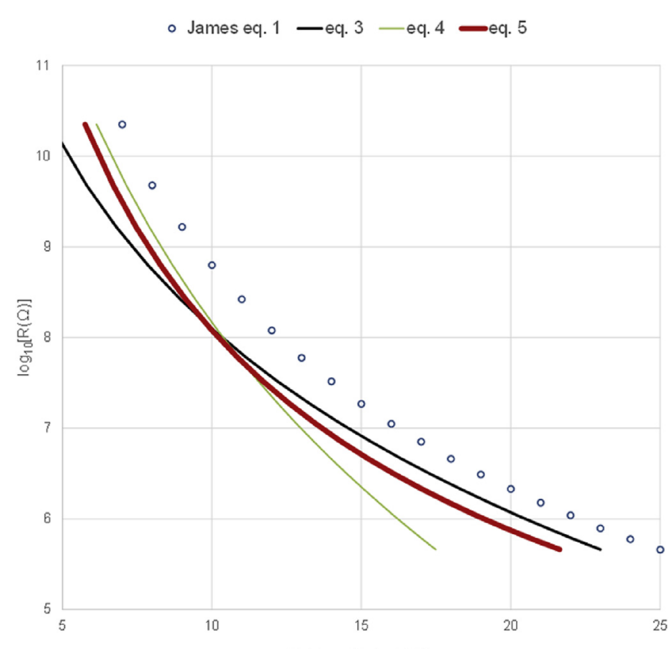

Fig. 2. Resistance vs moisture content given different correlations for OSB, with Douglas-fir reference [54].

Table 1
OSB sample conditions.

RH (%)	Temperature
35	26.6 °C
50	23 °C
65	26.6 °C
75	23 °C
88	23 °C
95	23 °C

different locations affects MC. The individual calculation methods and temperature corrections will be discussed below and evaluated against a set of OSB resistance data at representative MCs and temperatures. We also provide a new correlation and describe its advantages over other calculation methods. Finally, the data set was extended to cover OSB from different parts of North America to see the variation in OSB resistance regionally as different local tree species were used. This gives an initial indication of how much error one can expect from using a generic OSB correlation, compared to creating correlations specific to particular batches of OSB that might be used in one project. Of course more work needs to be done with OSB from other manufacturing locations to solidify a generic OSB correlation and the highest accuracy will generally result from testing individual OSB batches. We encourage further work evaluating OSB material variation and adoption of new correlation equation forms that are simple and accurate.

2. Materials and methods

2.1. Primary specimens

All the samples for the primary data set were cut from the same 1.2 m × 2.4 m × 11 mm (nominal 7/16″) thick OSB panel manufactured at a commercial mill in Michigan and obtained from a local building supplier. This OSB included wood from a mixture of tree species, primarily aspen (*Populus*), with some spruce (*Picea*), pine (*Pinus*), and a trace of basswood (*Tilia*). It had an oven-dry density of 534 ± 10 kg/m^3. Fifteen replicates each nominally 100 mm × 100 mm were placed in six different relative humidity (RH) chambers and left for over one month to condition to their equilibrium MC. Table 1 lists the conditions of each sample set. Two of the temperatures in that table, those at 26.6 °C, were not easily changed as these chambers were large conditioning rooms with a fixed temperature and RH used by multiple researchers. The goal was to reach different MC conditions in each sample set so a large range of resistance readings could be obtained, not to create a sorption isotherm. An additional twelve samples were first water soaked,[2] allowed to dry in a 50% RH room, and then six continued to condition in the 50% RH room while the other six were placed in an 88% RH chamber. These samples allowed comparison to the standard boards which all started their conditioning around 50% RH without being water soaked. Finally, an additional 10 specimens were conditioned at 60 °C and 80% RH. This supplemental data set allowed verification that the resistance temperature relationship explored below was not influenced by how the equilibrium MC conditions were achieved.

After reaching equilibrium 2.4 mm diameter holes were drilled using a standard jig with holes placed 31.8 mm on center. The electrodes placed into these holes were not standard moisture pins, but rather slotted hex washer head stainless steel 18-8 #6 × ½" sheet metal screws, similar to those used in Boardman et al. [58]. Insulating washers were placed below the hexagonal screw heads and in contact with the OSB surface so only the screw threads contact the wood. Between the insulating washer and the screw head was an uninsulated ring terminal crimped and soldered to lead wires connected to circuitry used to take the electrical resistance measurements. See Fig. 3 for a photograph of one specimen with screws and lead wires attached along with individual spare parts. When the screws were installed, a tight fit created electrical contact between the ring terminal and screw head. Note that this system allows finding the most conductive path through the wood at any depth but our equilibrated samples should not have had any moisture gradients. After installation of the screws and lead wires the samples were double wrapped in plastic bags with the lead wires carefully threaded out to minimize moisture transfer into or out of the sample while allowing resistance measurements to be taken at a variety of temperatures. Sets of these wrapped samples were then placed in temperature and humidity controlled chambers with the lead wires exiting the chamber. Resistance readings were taken at temperatures of −17, −5, 5, 23, 40, and 70 °C. Finally, the samples were removed from the plastic, screws removed, and a final mass check confirmed typically less than 0.2% mass change before and after resistance readings.

The resistance readings were taken with a voltage divider system capable of reading resistance up to 20 GΩ with less than 4% error, with a typical error of only 2% for lower resistances. A 10 V signal was applied to a circuit consisting of a reference resistor (from 200 kΩ to 10 MΩ) in series with the specimen, with voltage read across the reference resistor and resistance calculated for the specimen by voltage division. This system was automated to take 4 sequential readings with polarity of the applied voltage reversed between readings and the final resistance calculated as an average of the total four.

Gravimetric wood moisture content was calculated in the usual manner as the difference between the conditioned mass and oven-dry mass, divided by oven-dry mass. All specimens were oven-dried at 105 °C after resistance measurements were complete. The oven-dry specimen was considered stable after 18 h in the oven with a mass change between readings over 4 h apart typically less than 0.1% mass change, with maximum 0.28%. All specimens were weighed on a top loading balance with readability of 0.001 g. This procedure is similar to the secondary standard for oven-drying outlined in ASTM D4442-15 [64] which gives as a guide that "constant mass" is typically obtained within 24 h in the oven when

Fig. 3. Photograph of OSB specimen with screw and wire lead attachments.

[2] Similar to the procedure for any aqueous wood preservative treatment but here with water only, as used in Boardman et al. [42], the samples were placed in vacuum at 20 kPa for 30 min followed by pressurization with water at 1034 kPa for 60 min.

no appreciable change is noted in final mass at approximately 4 h intervals. In our case the typical change observed limits the MC accuracy to 0.2% and could not be improved without the much stricter mass measurement requirements in the primary standard.

2.2. Secondary specimens

Samples for the secondary data set were cut from 11 mm (nominal 7/16″) OSB sourced from Texas and British Columbia mills. Texas OSB samples were made from primarily southern yellow pine wood, and had an oven-dry density of 564 ± 19 kg/m^3. British Columbia OSB samples were made from primarily aspen wood (*Populus*), and had an oven-dry density of 565 ± 49 kg/m^3. Six replicates from each location were placed in the same conditions as Table 1 and prepared for resistance readings in the same manner as the primary data set. The temperatures sampled included −17, −5, 5, 10, 23, 40, and 60 °C. The 10 °C reading was added to be the lower temperature reading for the 50% RH readings. Very dry and cold samples reach resistance values too high for our equipment to measure reliably. The high temperature was reduced from 70 to 60 °C to improve the accuracy of MC estimate at high temperatures. When samples conditioned to high moisture content are raised to 70 °C a small amount of water leaves the sample and collects in the plastic bag, introducing an uncertainty in the actual MC of the sample. The reduced MC for some of the primary samples was estimated by comparing the initial and final mass of the sample after all temperature changes were completed. Reducing the maximum temperature to 60 °C eliminated this problem for the secondary data set. In the primary data set the MC at 70 °C was estimated as slightly below that of the other temperatures for select samples due to this issue, as shown the Appendix Table A.1 column for MC (%) at 70 °C. Otherwise the same procedures as the primary data set were used to measure resistance and final oven-dry mass.

2.3. Data analysis methods

Trends in the data were investigated in multiple ways. Linear and nonlinear models were used to understand the trends in the underlying data. Trend models in Table 2 were fit with a SAS® V9.4 [65] mixed model procedure (glimmix) to accommodate two sources of random variation (within and between specimens). Primary model fitting for the calibration equation is based on nonlinear inverse regressions to optimally predict moisture content. These fits were obtained with Microsoft Excel® Solver (GRG) with reduced weighting given to a few of the primary data sets to improve prediction. The squared residuals from −17 °C at 65% RH, −5 °C at 50% RH, and 5 °C at 30% RH were weighted by 50% to account for uncertainty in this data as resistances were very large. Overall model fits are based on comparisons of root-mean-square-error (RMSE) and visual assessments of the residuals. An equal weighted model was also fit for comparison of parameter estimates and calculation of the parameter estimates approximate standard errors (SE). It was fit with both the Excel solver and with the default Gauss-Newton nonlinear fitting routine in R [66].

3. Results

3.1. Basic trends

The basic trends are shown first for room temperature measurements. Fig. 4a indicates that OSB had a lower resistance than Douglas-fir at the same MC.

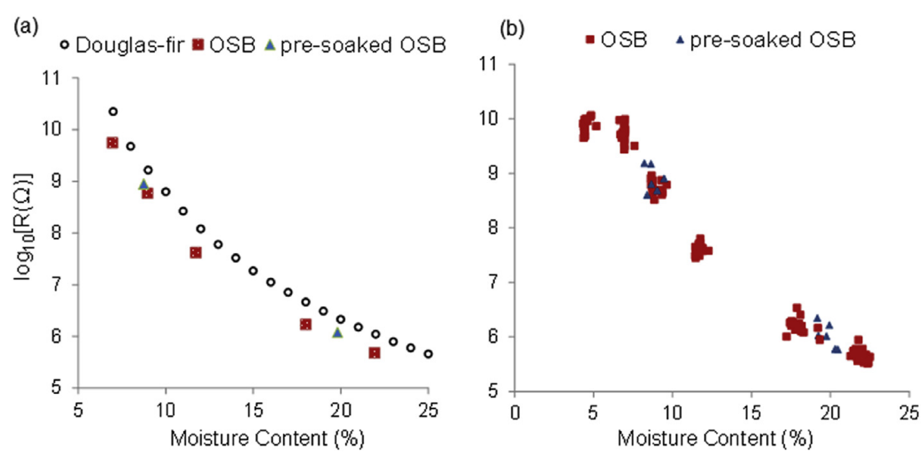

Fig. 4. a) OSB Resistance versus moisture content at room temperature, with Douglas-fir reference [54]. Each point for OSB represents the average of a group of specimens conditioned at a given relative humidity level. b) Resistance versus moisture content for all primary OSB samples at room temperature.

This is similar to plywood [58] and, again, suggests that the glue used in engineered wood products is more conductive than the wood, indicating that a different MC versus R correlation is needed. Fig. 4b presents all the primary OSB data points at room temperature to show the typical variations in reading. Unlike plywood, which had a higher resistance after water treatment and conditioning to a given moisture content, there was no significant difference in MC/R relationship between the pre-soaked samples and the standard OSB, despite the irreversible thickness swelling that occurs when OSB gets wet. The pre-soaked specimens reached higher equilibrium moisture content (EMC) than the non-soaked specimens conditioned at the same relative humidity, which is probably a result of sorption hysteresis. This does not matter to the results because resistance is correlated with MC rather than RH.

Similarly, the regional differences in OSB production due to different wood species had little effect on the resistance but changed the equilibrium MC somewhat. These trends are indicated in Figs. 5–7 where TX indicates OSB from Texas and BC indicates OSB from British Columbia while MI indicates the primary data set from Michigan. Fig. 5 is a summary of our resistance versus moisture content data for all three regions. Fig. 6 provides reference data from previous investigations of the sorption and

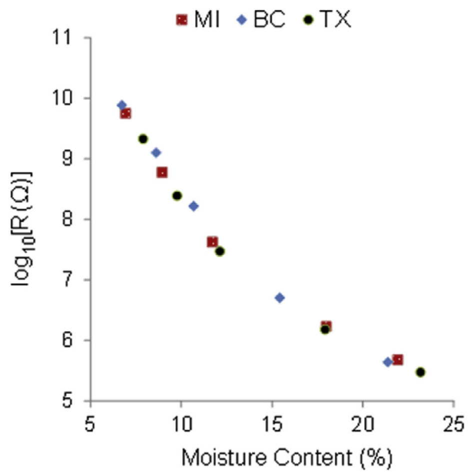

Fig. 5. Resistance versus moisture content for different sources of OSB.

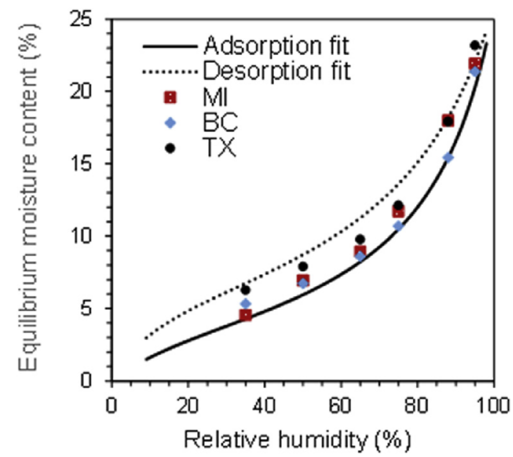

Fig. 7. Moisture Content versus relative humidity for different sources of OSB.

desorption EMC for OSB [67–75], along with best fit curves to each set. This compilation of literature data indicates that the hygroscopicity of OSB can vary considerably, since the moisture sorption isotherms show considerable variation in equilibrium MC at given RH. Fig. 7 plots our summary data from the three regions over the fits of EMC versus RH from the reference data. The direction of sorption (adsorption vs. desorption) in our measurements was not strictly controlled; specimens were placed in various RH conditions as received and prior history was not known. Again, the goal of this work was to enhance the understanding of temperature effects on resistance readings across a range of MC values, not to investigate the sorption isotherm. Our EMC values generally fall between the reference adsorption and desorption curves, with OSB from the Texas mill typically having higher EMC than OSB from the Michigan and British Columbia mills. The reference figures and comparison to our data were provided to show that our three different sample locations have EMC behavior similar to previous investigations.

3.2. Temperature effects

The results become more complicated when temperature effects are included. Fig. 8 is a plot of the logarithm of resistance versus inverse temperature. It shows the resistance decreased as the temperature increased, but the temperature is plotted as 1000 divided by the temperature in Kelvin to create an upward sloping set of graphs at constant MC. EMC is indicated in the legend on top, and linear fit lines are applied to the data points to indicate overall trends.

Fig. 8a includes the average resistance of the additional 10 specimens in the supplemental set conditioned at 60 °C and 80% RH, which are indicated by the open black triangles at 12.8%MC and behave similarly to the 11.7%MC of the standard 75% RH samples. Fig. 8b presents the secondary data sets and indicates the temperature trends are not significantly different from the primary set. Note that, while a linear fit appears to work well, the slopes are different for different MCs based on a multilevel linear model of the sets of the specimens (excluding some observations where measured resistance had a large uncertainty). Each separate location (MI, BC, TX) was treated as a set with one common non-zero intercept and then the slope was determined for each subset of MCs. The hypothesis that the MC slopes were identical within each separate location was rejected ($p < 0.0001$). Although the models allow correlation within each specimen, the residuals indicate some nonlinearities not accommodated by the simple models. The data in Fig. 8 appear nonlinear with downward curvature at low moisture content but with upward curvature at high moisture content. Table 2 presents the slopes of linear fits, with common non-zero intercept within each group, to data in Fig. 8 showing increasing slope with decreasing MC. Precision estimates for the slope coefficients are given in Table 2 by the standard errors (SE); they are derived as a function of both the between and within specimen errors within each group. The nonzero intercepts are estimated as −3.12 with standard error (SE) = 0.081 for MI, −3.23 with SE = 0.107 for BC, and −3.89 with SE = 0.142 for TX. The full

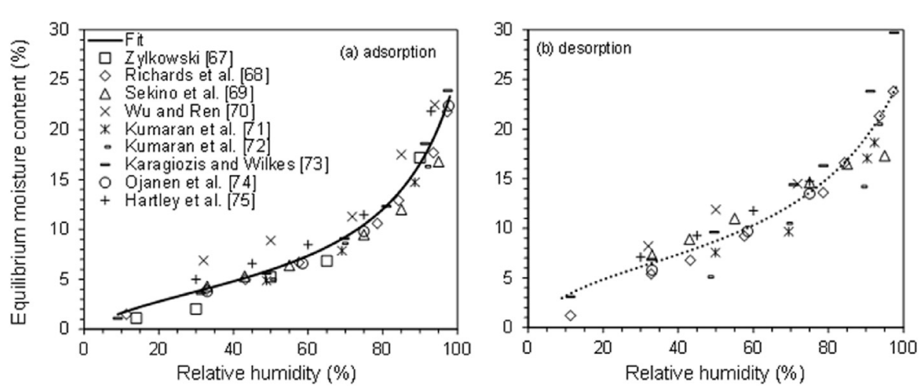

Fig. 6. OSB adsorption (a) and desorption (b) data from literature along with best fit curves.

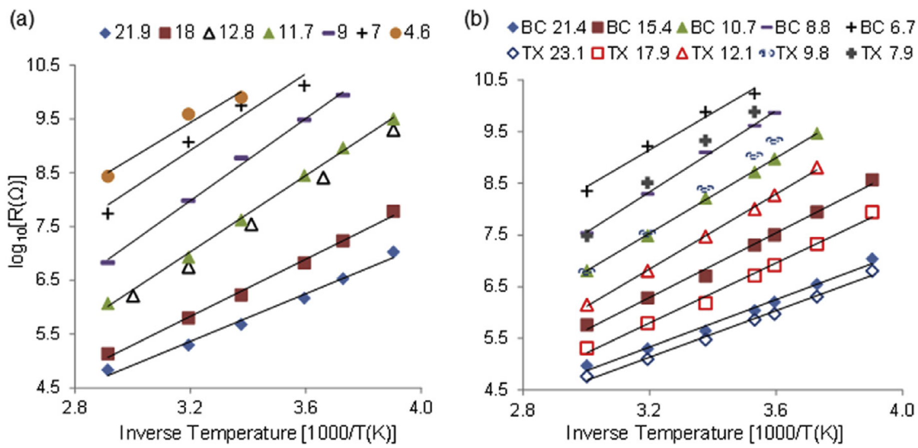

Fig. 8. OSB $\log_{10}$ R versus 1000/temperature. a) MI Primary set, b) BC and TX secondary set.

data set of resistance and temperature measurements for all samples is provided in Appendix A.

Table 2
Slope for $\log_{10}$ R vs Inverse Temperature (1000/K) in Fig. 8.

Origin	Moisture content (%)	Slope	±SE
MI	21.9	2.61	0.025
	18	2.78	0.025
	12.8	3.13	0.026
	11.7	3.20	0.025
	9	3.48	0.026
	7	3.75	0.026
	4.6	3.93	0.028
BC	21.4	2.64	0.032
	15.4	2.99	0.032
	10.7	3.38	0.033
	8.8	3.63	0.033
	6.7	3.86	0.034
TX	23.1	2.77	0.043
	17.9	3.01	0.043
	12.1	3.37	0.045
	9.8	3.63	0.045
	7.9	3.87	0.046

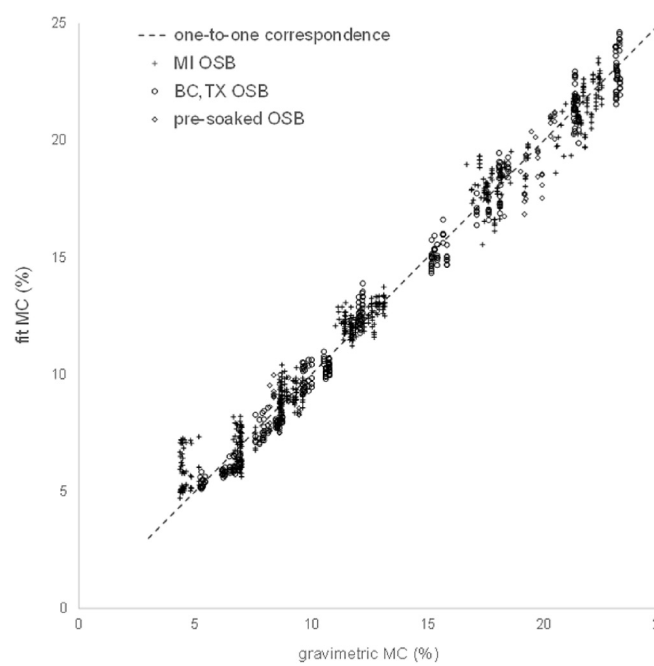

Fig. 9. Eq. (2) correlation fit moisture content versus gravimetric moisture content for all data.

3.3. Calibration equation

Our primary interest was in creating a correlation that allowed calculation of MC from resistance and temperature data in OSB. See Eq. (2) for our preferred form where b_x are fit coefficients, T_f represents 1000 divided by temperature in Kelvin, and R is the resistance in ohms.

$$MC = b_0 + b_1 T_f^{b_4} + b_3 T_f^{b_4} \log_{10}[\log_{10}(R) - b_2] \quad (2)$$

The form of this equation was chosen for simplicity and ease of calculation, just including the terms that help to create a good correlation with a small nod to the underlying physics which is hinted at in the use of the inverse temperature and the log function commonly used in these correlations. We provide all our data in case someone wants to try a more complex calculation that better reflects the underlying physics. As discussed below other correlations also work satisfactorily, but are unnecessarily complicated. For this equation form a global optimization across both the primary and secondary data sets, including the pre-soaked samples, yields fit coefficients $b_0 = -8.6810$, $b_1 = 3.7172$, $b_2 = 3.8974$, $b_3 = -2.9129$, $b_4 = 1.9000$. This results in an overall root-mean-square-error (RMSE) of 0.726 in %MC for MC across the total sample size of 1001 measurements. Fig. 9 shows the fit MC versus the gravimetric MC for this correlation for all 1001 data points. Fig. 10 presents a different view of the data scatter by plotting resistance versus moisture content comparing the fit from Eq. (2) to the gravimetric MC at three different temperatures.

Another indication that this correlation is robust can be seen in Table 3 which shows the optimized fit coefficients for each of four subsets of the data, along with two versions of the RMSE, one using the subset optimized fit and the other using the overall fit. The first row indicates the overall fit from the full data set. The subsequent rows fit the Primary set (MI), just the water-soaked (pre-soak), the British Columbia set (BC) and the Texas set (TX). The final lines in Table 3 show fit coefficients and their associated approximate standard errors using the R statistical software package to optimize Eq. (2) on an equally weighted data set. Small standard errors relative to the coefficient estimates are indicative of more precise parameter estimates. Recall that the other

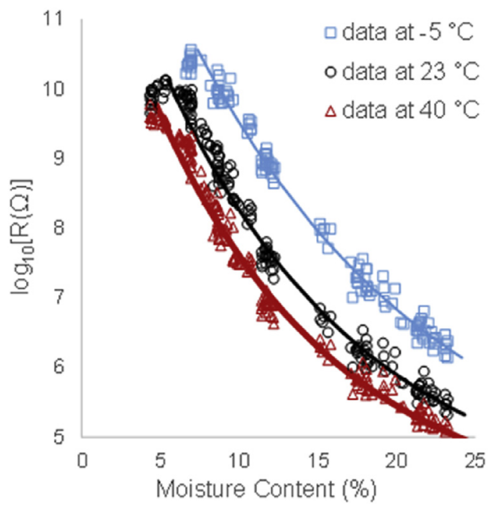

Fig. 10. Resistance versus gravimetric moisture content at three temperatures showing curve fits (Eq. (2)).

correlation parameters reduce the weight of select data sets with high resistance as described in the data analysis methods section above. By going to a combined five-parameter model, versus separate models for each group, the subsets experience modest increases in their RMSE with the exception of the BC subset, which experiences a 35% increase in RMSE under the overall fit. Although statistically significant, it still does not exceed the error within each of the other subsets.

3.4. Comparison to previous correlations

In this section we show the results of running three different previously used OSB correlations against our full data set, both as given and as optimized for this data set. This state of the art survey suggests the need for a simplified equation form like Eq. (2). The calculation formulas shown below were modified to include 5 optimization coefficients, to allow a fair comparison to Eq. (2). In each case these equations use the temperature in °C, represented as T. They also often use the natural log, denoted by ln(), or e raised to a power, denoted by exp(). The first case is that outlined by a manufacturer of moisture pins and data acquisition equipment (private communication), which uses formulas from both Maref [59] and Garrahan [56] in a string of calculations shown as Eq. (3).

$$MC_u = \exp[b_0 - b_1 \ln(R/1000)]$$
$$MC_t = \frac{MC_u + 0.567 - 0.026T + 0.000051T^2}{0.881 \times 1.0056^T} - b_2 \qquad (3)$$
$$MC = 100 \times \exp[b_3 \ln(MC_t/100) + 0.001187 b_4]$$

As given $b_0 = 4.0954$, $b_1 = 0.14006$, and $b_3 = 1.055$ with the other fit coefficients not used ($b_2 = 0$, $b_4 = 1$). This results in a RMSE of 1.7 on our data set. Our optimized fit using all fit coefficients improves the RMSE to 0.927 as shown in Table 4.

The second case is taken from a paper by Carll et al. [5] which makes only a modest effort to include the temperature effects by assuming a constant straight-line relationship between natural log of resistance and temperature. This is shown in Eq. (4).

$$MC = \exp\{b_0 + b_1[b_3 \ln(R) - b_2(21 + b_4 - T)]\} \qquad (4)$$

As given $b_0 = 4.170$, $b_1 = -0.097$, and $b_2 = 0.0792$ with other fit coefficients not used ($b_3 = 1$, $b_4 = 0$). This results in a RMSE of 2.29 for our data set. Our optimized fit using all fit coefficients improves the RMSE to 1.04 as shown in Table 4. Finally the third case is taken from Straube's field guide [52] and is shown in Eq. (5).

$$MC_u = 10^{b_0 - b_1 \log_{10}[\log_{10}(R) - b_2]}$$
$$MC = \left(\frac{MC_u + 0.567 - 0.026T + 0.000051T^2}{0.881 \times 1.0056^T} - b_4\right) \Big/ b_3 \qquad (5)$$

As given $b_0 = 2.990$, $b_1 = 2.113$, $b_2 = 0$ is not used, $b_3 = 1.1114$, and $b_4 = 0.366$. This results in a RMSE of 1.52 for our data set. Our optimized fit using all fit coefficients improves the RMSE to 0.773 as shown in Table 4.
Fig. 11 plots the optimized fit for each equation against the data for two temperatures, similar to Figs. 2 and 10, to illustrate the improvement provided by Eq. (2).

4. Discussion

Clearly the influence of temperature on moisture pin resistance is significant and complex. Fig. 8 is similar to Arrhenius plots which typically show the effect of temperature on rates of chemical reactions, with the slope proportional to the activation energy for the reaction. A similar interpretation can be applied to our data: the activation barrier for charge carrier conduction (proportional to the slope) decreases as moisture content increases. Non-linearity was evident, however, in these Arrhenius plots, and curvature was in different directions at low and high moisture content. This may be an indication that different conduction mechanisms are at work in low and high moisture regimes.

In this work we publish all our OSB data and compare our suggested correlation to existing formulas to inspire further work. We suggest that building science researchers pay closer attention to the temperature correction, folding it into the base correlation that relates resistance to moisture content, not treating it as an afterthought. Many of the current correlations in use are overly complex, even if they are accurate enough for most purposes. Our suggested correlation (Eq. (2)) has enough complexity that it can handle the wide temperature range we explored, yet can be written in one line. It uses the more fundamental absolute temperature in Kelvin thus avoiding negative numbers and allowing the fit to use fractional powers of the temperature. It also contains a cross term

Table 3
Fit coefficients and RMSE for various data subsets.

Data	n	Overall RMSE	Subset optimized	b_0	b_1	b_2	b_3	b_4
Full	1001	0.726		**−8.6810**	**3.7172**	**3.8974**	**−2.9129**	**1.9000**
MI	545	0.754	0.731	−8.7427	3.5252	3.9101	−2.7992	1.9465
Pre-soak	72	0.949	0.804	−38.6449	39.2631	1.1845	−22.7684	0.7433
BC	192	0.601	0.445	−16.6093	9.3989	3.7188	−6.0133	1.3177
TX	192	0.661	0.612	−7.5852	2.7011	4.1152	−2.0905	2.0789
Equal weight		0.765		−7.6192	3.2420	3.8947	−2.6262	1.9913
Standard error				0.8252	0.4271	0.0569	0.2989	0.0799

Table 4
Fit coefficients and RMSE for various calculation methods.

Method	As given RMSE	Optimized RMSE	b_0	b_1	b_2	b_3	b_4
Eq. (2)		0.726	−8.6810	3.7172	3.8974	−2.9129	1.9000
Eq. (3)		0.927	3.8786	0.0893	5.6819	1.0176	1.0667
	1.7		4.0954	0.1401	0	1.0550	1
Eq. (4)		1.04	4.8165	−0.1349	0.0704	0.9543	−2.8194
	2.29		4.1700	−0.0970	0.0792	1	0
Eq. (5)		0.773	2.5607	1.3322	0.0000	1.1935	9.8660
	1.52		2.9900	2.1130	0	1.1114	0.3660

with both temperature and resistance, improving accuracy. It is suggested that future work include an even better mathematical form to capture the complex physics governing charge carriers in wood and wood composites. Meanwhile, Eq. (2) has reduced the RMSE compared to commonly used correlations.

Further evidence for the importance of temperature correction can be demonstrated by fitting Eq. (5) without the benefit of the full data set. Fitting all parameters to only the resistance data at room temperature yields an overall RMSE of 1.173 ($b_0 = 2.274$, $b_1 = 1.108$, $b_2 = 0$ is not used, $b_3 = 0.822$, and $b_4 = 9.847$). The rest of the reduction to RMSE of 0.773 is only accomplished when using the full data set with temperature variations. This suggests that the temperature correction for OSB differs from that for solid wood, for which Eq. (5) was originally developed. Also note that the fit parameters that control temperature have moved considerably as b_4 changes from less than 1 as originally given to near 10. One of the motivations for developing Eq. (2) was to allow a more robust calculation on diverse data sets.

The robustness of our preferred correlation has yet to be fully demonstrated, but the variability in the MC/T/R relationship for OSB panels from different geographic locations sampled in this study could be handled by a single calibration equation. The overall fit for the full data set resulted in a RMSE of less than 1% MC when applied to the full data set as well as all subsets,

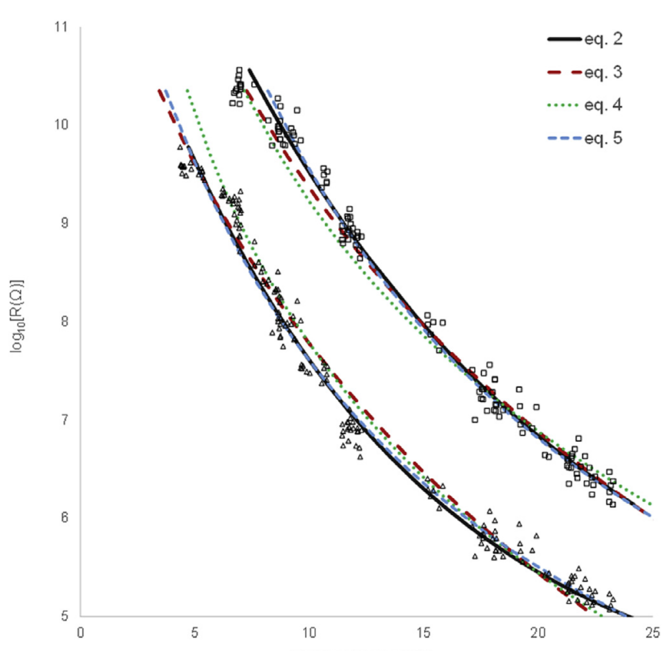

Fig. 11. Comparison of optimized correlations at −5 °C (upper set) and 40 °C (lower set).

implying that variability across the panels from different mills was not appreciably greater than within-panel variability (Table 3). This correlation should enhance the field evaluation of the hygrothermal performance of wall and roof assemblies that use OSB. Nonetheless, it would be helpful to have further verification that OSB from different locations can be accounted for in a generic OSB correlation without introducing significant error. The inherent variability of wood and different OSB manufacturing techniques will always mean that moisture pin methods are less accurate than direct gravimetric measurement for determination of moisture content. Yet the practical advantages of moisture pins for field investigation will drive continued efforts to improve this method.

5. Conclusion

Samples of commercial OSB from mills in three different regions in North America were conditioned to a range of moisture contents in equilibrium with relative humidity levels from 35% RH to 95% RH at room temperature. These samples were then subjected to a wide range of temperatures (−17 to 70 °C) at which the resistance between a set of moisture pins was measured. The samples were then oven-dried to obtain the gravimetric moisture content and a correlation was developed to allow prediction of the moisture content given the resistance and temperature readings. The proposed correlation (Eq. (2)) is more concise and has a better root-mean-square-error than other commonly used correlations. It allows for a more accurate determination of moisture content in OSB and covers a wide temperature range making it useful for field investigations.

Acknowledgments

This manuscript was improved by comments from Marshall Begel and Laura Hasburgh of the USDA Forest Products Laboratory (FPL), and anonymous reviewers. The writers gratefully acknowledge the help of many FPL colleagues during the course of this investigation, including Robert Munson, Alex Wiedenhoeft, and Laurice Spinelli.

Research was funded by the Forest Products Laboratory of the U.S. Forest Service. This research was performed by U.S. government employees on official time and is therefore in the public domain and not subject to copyright.

Appendix

Table A.1
Primary data set.

Sample	MC (%)	MC (%) at 70 °C	Resistance (MΩ) −17 °C	−5 °C	5 °C	23 °C	40 °C	70 °C
1	17.9	17.4	143	36.5	14.0	3.43	1.19	0.270
2	19.2	18.6	48.6	13.8	5.71	1.46	0.553	0.116
3	17.5	16.9	75.5	20.7	8.04	1.93	0.686	0.150
4	17.8	17.2	42.9	12.4	4.95	1.35	0.500	0.120
5	19.3	18.6	24.3	7.40	3.22	0.884	0.362	0.0819
6	17.6	17.0	72.5	20.6	7.78	1.89	0.694	0.144
7	18.0	17.3	64.9	19.1	7.23	1.75	0.623	0.140
8	18.1	17.4	41.7	12.3	4.94	1.26	0.472	0.111
9	17.2	16.7	34.8	10.0	3.91	1.01	0.414	0.0942
10	17.4	16.9	66.6	19.4	7.24	1.81	0.666	0.127
11	18.1	17.5	95.0	25.8	9.59	2.53	0.953	0.191
12	18.3	17.7	37.6	10.8	4.39	1.22	0.469	0.109
13	18.2	17.6	47.2	14.1	5.66	1.58	0.627	0.147
14	17.5	16.9	57.6	16.5	6.47	1.60	0.557	0.125
15	17.6	17.0	56.1	16.2	6.65	1.71	0.632	0.119
16	7.0	7.0		26000	10900	6280	1360	78.9
17	6.9	6.9		32000	16400	8050	1760	99.4
18	6.8	6.8		22400	9070	4500	981	37.6
19	7.0	7.0		26000	10800	4230	740	36.5
20	7.0	7.0		16500	10300	3130	522	20.1
21	7.0	7.0		24500	15700	5680	972	44.7
22	6.9	6.9		20300	10100	3610	903	31.1
23	7.0	7.0		36500	12800	2730	755	26.5
24	6.9	6.9		29400	13400	5400	1480	84.4
25	7.0	7.0		23300	15400	9740	2140	92.5
26	6.8	6.8		23500	17500	5640	1080	52.0
27	7.6	7.6		26000	13500	3180	660	26.9
28	6.7	6.7		16700	14200	9440	1740	58.0
29	7.0	7.0		25200	14000	7190	1290	76.0
30	6.7	6.7		21400	12300	5100	1240	51.4
31	8.7	8.7	9380	7140	3110	530	72.0	5.12
32	8.6	8.6	16000	9740	3710	814	108	7.49
33	8.7	8.7	14500	11000	3550	679	95.0	6.73
34	8.7	8.7	17500	8660	3220	651	85.8	6.10
35	8.9	8.9	15500	6360	2460	325	56.3	3.86
36	9.3	9.3	17200	8460	3230	741	114	8.18
37	9.4	9.4	10300	6440	2180	449	68.1	5.41
38	8.7	8.7	17400	7240	2790	434	69.4	5.75
39	9.2	9.2	16600	9280	2590	501	94.6	6.30
40	8.6	8.6	17700	9210	2670	606	101	6.53
41	9.3	9.3	15100	7900	2890	409	66.0	5.08
42	8.8	8.8	12200	15600	3120	739	110	7.66
43	8.7	8.7	22200	9710	4630	908	183	11.4
44	9.6	9.6	15100	7010	2850	614	103	7.92
45	8.9	8.9	14700	6240	2520	472	91.6	6.49
46	4.5	4.5			13600	4850	3770	321
47	4.8	4.8			14700	10800	4170	251
48	5.2	5.2			12700	7310	3160	191
49	4.8	4.8			16700	11500	3610	260
50	4.5	4.5			14200	9810	3870	287
51	4.4	4.4			16600	5830	3960	301
52	4.6	4.6			16100	8910	3090	232
53	4.5	4.5			20600	9170	3770	247
54	4.4	4.4			14600	5970	3890	280
55	4.5	4.5			16700	6650	3810	284
56	4.4	4.4			14300	7090	3900	295
57	4.4	4.4			26700	9730	3250	267
58	4.4	4.4			24600	8090	6010	299
59	4.5	4.5			16300	8880	3800	242
60	4.4	4.4			16400	4470	3960	313
61	11.8	11.4	3840	1410	429	63.0	12.9	1.72
62	11.7	11.4	3960	1180	354	51.1	9.59	1.19
63	11.9	11.7	2580	894	280	42.8	9.59	1.27
64	11.8	11.4	3660	1160	362	53.1	10.5	1.50
65	11.5	11.2	3060	828	269	39.0	7.72	1.08
66	11.8	11.5	3330	995	298	41.8	7.93	1.09
67	11.7	11.3	2600	687	210	30.9	6.14	0.831
68	11.5	11.2	2960	629	189	28.1	5.50	0.832
69	11.7	11.3	3600	1120	342	48.8	9.50	1.18
70	11.4	11.2	2590	682	207	30.9	6.97	0.924
71	11.4	11.0	2910	946	293	44.9	9.12	1.25
72	12.3	11.9	2980	738	238	38.0	7.97	1.10
73	11.9	11.6	3570	768	244	37.4	8.29	1.14
74	11.7	11.4	3230	807	259	39.8	8.16	1.13
75	11.8	11.5	2700	849	264	40.0	8.42	1.33
76	21.6	21.2	15.7	5.04	2.09	0.601	0.259	0.0856
77	21.3	20.3	10.8	3.42	1.48	0.445	0.178	0.0597
78	22.1	21.0	6.84	2.26	1.02	0.337	0.140	0.0526
79	22.4	21.3	6.77	2.19	0.973	0.338	0.141	0.0516
80	22.5	21.3	7.96	2.65	1.21	0.432	0.181	0.0619
81	21.9	20.6	10.5	3.36	1.46	0.481	0.199	0.0712
82	21.5	20.6	13.3	4.11	1.80	0.536	0.260	0.0779
83	22.4	21.3	5.22	1.74	0.869	0.328	0.132	0.0483
84	22.4	21.4	8.29	2.58	1.08	0.383	0.165	0.0586
85	21.5	20.6	13.7	4.29	1.80	0.556	0.229	0.0774
86	21.7	20.8	8.62	2.84	1.24	0.417	0.176	0.0633
87	21.8	20.5	20.2	6.47	2.67	0.878	0.309	0.103
88	22.2	21.3	10.3	3.26	1.39	0.478	0.191	0.0689
89	21.7	20.8	7.96	2.57	1.10	0.366	0.148	0.0561
90	22.1	20.9	13.6	4.30	1.90	0.601	0.242	0.0861
W1	8.2	8.2	19800	11200	9690	1530	268	19.1
W2	8.4	8.4	13400	6230	2390	403	77.9	8.22
W3	8.6	8.6	19000	18800	7580	1500	324	26.7
W4	9.0	9.0	14800	8010	2550	486	97.9	7.40
W5	8.7	8.7	13300	8570	3350	635	125	9.80
W6	9.5	9.5	17000	14200	3970	802	164	12.7
W7	20.3	19.5	14.0	4.40	1.97	0.606	0.268	0.0672
W8	20.5	19.7	13.3	4.22	1.83	0.593	0.278	0.0711
W9	19.7	19.0	26.7	8.26	3.67	1.04	0.474	0.102
W10	19.2	18.5	30.4	9.00	3.87	1.06	0.465	0.102
W11	19.2	18.3	66.6	20.4	8.36	2.23	0.878	0.179
W12	19.9	19.2	43.1	13.6	5.58	1.66	0.665	0.141

Table A.2
Supplemental data set.

Sample	MC (%)	Resistance (MΩ) −17 °C	0 °C	20 °C	40 °C	60 °C
H1	12.7	3630	504	65.7	9.47	2.74
H2	12.8	1660	212	28.8	4.77	1.38
H3	13.1	1690	219	31.2	5.65	1.62
H4	12.5	2270	303	40.5	6.09	1.82
H5	12.6	1640	212	28.9	4.94	1.43
H6	12.6	2580	322	42.7	6.69	1.90
H7	12.9	1500	199	27.7	4.70	1.40
H8	12.8	1740	217	29.3	4.79	1.42
H9	13.1	1230	161	23.0	3.79	1.19
H10	13.2	1820	213	28.1	4.91	1.41

Table A.3
Secondary data set.

Sample	MC (%)	Resistance (MΩ) −17 °C	−5 °C	5 °C	10 °C	23 °C	40 °C	60 °C
BC 1	15.7	226	51.2	19.9	12.5	3.18	1.27	0.388
BC 2	15.2	384	93.5	31.8	20.6	4.85	1.97	0.572
BC 3	15.2	480	116	40.9	26.6	7.05	2.54	0.759
BC 4	15.3	337	74.3	28.3	18.3	4.43	1.68	0.496
BC 5	15.8	402	97.7	33.6	21.8	5.41	2.14	0.652
BC 6	15.4	410	98.9	34.5	22.0	5.35	1.93	0.576
BC 7	6.7				15400	7210	1880	267
BC 8	6.5				17500	8410	1700	233
BC 9	6.9				20000	8280	1600	202
BC 10	6.7				17300	7700	1720	232
BC 11	6.9				16300	6060	1430	186
BC 12	6.7				17000	8140	1600	222
BC 13	8.7			6350	3560	1100	158	26.6
BC 14	8.6			7810	4820	1350	209	38.3
BC 15	8.8			6610	3420	1090	177	33.2
BC 16	8.5			7600	4010	1330	203	35.7
BC 17	8.6			7550	4050	1340	214	35.6
BC 18	8.5			8030	4900	1370	217	38.6

Table A.3 (*continued*)

Sample	MC (%)	Resistance (MΩ)						
		−17 °C	−5 °C	5 °C	10 °C	23 °C	40 °C	60 °C
BC 19	5.3					13400	3380	560
BC 20	5.2					11700	3400	579
BC 21	5.4					11400	2760	441
BC 22	5.3					9080	3660	620
BC 23	5.3					13000	3450	562
BC 24	5.4					13200	2940	493
BC 25	10.8		2660	852	487	153	29.3	6.18
BC 26	10.6		3650	1200	665	218	38.8	8.08
BC 27	10.5		2320	717	398	114	23.7	4.51
BC 28	10.6		3120	1030	570	177	33.7	6.96
BC 29	10.8		2590	788	440	136	25.6	5.39
BC 30	10.8		3380	1100	608	194	35.4	7.77
BC 31	21.5	10.1	3.28	1.52	0.999	0.423	0.181	0.0894
BC 32	21.4	6.68	2.24	1.05	0.736	0.305	0.143	0.0682
BC 33	21.3	11.9	3.84	1.74	1.22	0.487	0.221	0.0983
BC 34	21.3	12.8	3.98	1.77	1.17	0.457	0.214	0.101
BC 35	21.4	9.63	3.32	1.47	0.982	0.420	0.188	0.0954
BC 36	21.5	14.4	4.52	2.05	1.45	0.556	0.247	0.112
TX 1	17.1	143	32.3	12.0	7.60	1.92	0.826	0.256
TX 2	17.6	126	30.0	11.6	7.34	2.06	0.852	0.281
TX 3	18.5	46.7	12.6	4.99	3.21	1.03	0.410	0.142
TX 4	18.1	107	26.0	10.0	6.35	2.02	0.745	0.251
TX 5	18.1	47.6	12.6	4.91	3.17	0.96	0.402	0.139
TX 6	18.1	55.5	14.5	5.67	3.59	1.12	0.471	0.161
TX 7	8.0				5850	1670	257	26.9
TX 8	8.0				7700	2250	353	35.8
TX 9	7.9				7750	2210	323	28.9
TX 10	8.1				6350	1530	244	24.2
TX 11	7.8				9500	2630	405	36.4
TX 12	7.6				8700	2420	377	30.7
TX 13	9.7			2300	1160	269	36.8	6.78
TX 14	9.6			2350	1200	262	34.1	6.05
TX 15	9.7			2090	1090	247	33.6	6.1
TX 16	9.7			2080	1060	246	35.7	6.6
TX 17	10.0			1780	939	212	30.1	5.6
TX 18	9.9			2050	1040	232	31.1	5.6
TX 19	6.3					8940	2080	304
TX 20	6.3					7330	1960	284
TX 21	6.5					8260	1810	230
TX 22	6.2					8270	1950	274
TX 23	6.2					8740	1920	254
TX 24	6.2					9480	2250	318
TX 25	12.1		715	214	118	32.6	7.67	1.69
TX 26	12.1		749	218	122	36.2	7.69	1.66
TX 27	12.2		441	123	60.0	18.8	4.24	0.931
TX 28	12.1		818	240	131	39.6	8.31	1.85
TX 29	12.2		537	153	76.2	25.3	5.24	1.14
TX 30	12.0		604	172	95.8	24.5	5.48	1.23
TX 31	23.1	9.43	2.96	1.32	1.02	0.409	0.171	0.0751
TX 32	23.2	6.91	2.16	0.974	0.757	0.302	0.131	0.0583
TX 33	23.3	7.38	2.38	1.10	0.881	0.348	0.150	0.0689
TX 34	23.3	4.28	1.38	0.637	0.491	0.209	0.0879	0.0418
TX 35	23.1	5.84	1.86	0.922	0.687	0.294	0.119	0.060
TX 36	23.1	4.64	1.47	0.699	0.528	0.229	0.0983	0.0466

References

[1] J.I. Zerbe, Z. Cai, G.B. Harpole, An Evolutionary History of Oriented Strandboard (OSB), Forest Products Laboratory, Madison, WI., 2015. FPL-GTR-236.

[2] C. Carll, A. Wiedenhoeft, Moisture-related properties of wood and the effects of moisture on wood and wood products, in: Moisture Control in Buildings: the Key Factor in Mold Preventions, seco[nd] ed., ASTM International, 2009. MNL 18.

[3] L. Haughton, C. Murphy, "Moisture exchange": performance of OSB and plywood structural panels, Interface (June 2003) 6–13. Available online at, http://suncrestshed.com/Plywood-OSB.pdf.

[4] D. Cautley, Comparative measured moisture performance of wood-frame walls, in: Proceedings, Wood-frame Housing Durability and Disaster Issues, Forest Products Society, Madison, WI, 2004, pp. 201–209.

[5] C. Carll, A. TenWolde, R. Munson, Moisture performance of a contemporary wood-frame house operated at design indoor humidity levels, in: Proceedings, Thermal Performance of Exterior Envelopes of Whole Buildings X, Clearwater Beach, FL, ASHRAE, Atlanta, GA, Dec. 2-7, 2007. ORNL 07-Go1409/aas.

[6] S.D. Gatland II, A.N. Karagiozis, C. Murray, K. Ueno, The hygrothermal performance of wood-framed wall systems using a relative humidity-dependent vapor retarder in the Pacific Northwest, in: Proceedings, Thermal Performance of the Exterior Envelopes of Whole Buildings X International Conference, Clearwater Beach, FL, USA, 2007.

[7] R. Tichy, C. Murray, Developing Innovative Wall Systems that Improve Hygrothermal Performance of Residential Buildings, Final Report to U.S. Department of Energy, 2007.

[8] J. Wilkinson, K. Ueno, D. De Rose, J.F. Straube, D. Fugler, Understanding vapour permeance and condensation in wall assemblies, in: Proceedings of the 11th Canadian Conference on Building Science and Technology, Banff, Alberta, 2007.

[9] C.J. Schumacher, Hygrothermal Performance of Insulated, Sloped, Wood-Framed Roof Assemblies, Master's Thesis, Department of Civil Engineering, University of Waterloo, Ontario, Canada, 2008.

[10] M.M. Armstrong, W. Maref, M. Rousseau, W. Lei, M. Nicholls, A field monitoring study of interstitial condensation in wood-frame walls in cold climate, in: Proceedings of the 12th Canadian Conference on Building Science and Technology, Montréal, Quebec, May 6-8, 2009.

[11] S.C. Drumheller, C.G. Carll, Effect of cladding systems on moisture performance of wood-framed walls in a mixed-humid climate, in: Proceedings, Thermal Performance of the Exterior Envelopes of Whole Buildings XI International Conference, Clearwater Beach, FL, USA, 2010.

[12] S. Yuan, A.N. Karagiozis, The hygrothermal performance of wood-framed wall systems using spray polyurethane foam insulations and a smart vapor retarder in the Pacific Northwest, in: Proceedings, Thermal Performance of the Exterior Envelopes of Whole Buildings XI International Conference, Clearwater Beach, FL, USA, 5–9 December 2010.

[13] T.A. Weston, L.C. Minnich, Moisture measurements and condensation potential in wood frame walls in a hot-humid climate, J. Test. Eval. 39 (2011) 395–409.

[14] L.B. Arena, D. Owens, P. Mantha, Measured performance of an R-40 double-stud wall in climate zone 5a, in: Proceedings, Thermal Performance of the Exterior Envelopes of Whole Buildings XII International Conference, Clearwater Beach, FL, USA, 1–5 December 2013.

[15] A. Grin, J. Smegal, J. Lstiburek, Application of Spray Foam Insulation under Plywood and Oriented Strand Board Roof Sheathing, Building America Report 1312, Building Science Corporation, Somerville, MA, USA, 2013.

[16] G. Parsons, B. Lieburn, Comparative energy and wall performance of twelve residential houses constructed in a cold climate, in: Proceedings, Thermal Performance of the Exterior Envelopes of Whole Buildings XII International Conference, Clearwater Beach, FL, USA, 1–5 December 2013.

[17] J. Smegal, J. Lstiburek, J. Straube, A. Grin, Moisture-related durability of walls with exterior insulation in the Pacific Northwest, in: Proceedings, Thermal Performance of the Exterior Envelopes of Whole Buildings XII International Conference, Clearwater Beach, FL, USA, 1–5 December 2013.

[18] C. Craven, R. Garber-Slaght, Exterior insulation envelope retrofits in cold climates: implications for moisture control, HVAC R Res. 20 (2014) 384–394.

[19] M. Fox, J. Straube, H. Ge, T. Trainor, Field test of hygrothermal performance of highly insulated wall assemblies, in: Proceedings of the 14th Canadian Conference on Building Science and Technology, Toronto, Canada, 28–30 October 2014, pp. 101–110.

[20] HIRL, Moisture Performance of Walls in Energy Efficient Homes, Home Innovation Research Labs, Upper Marlboro, MD, 2014. Report 5932.001_08142014.

[21] S.V. Glass, V. Kochkin, S.C. Drumheller, L. Barta, Moisture performance of energy −efficient and conventional wood-frame wall assemblies in a mixed-humid climate, Buildings 5 (2015) 759–782, http://dx.doi.org/10.3390/buildings5030759.

[22] K. Ueno, Monitoring of Double-Stud Wall Moisture Conditions in the Northeast, Building America Report 1501, Building Science Corporation, Westford, MA, USA, 2015.

[23] K. Ueno, J.W. Lstiburek, Field Testing Unvented Roofs with Asphalt Shingles in Cold and Hot-Humid Climates, Building America Report 1409, Building Science Corporation, Westford, MA, USA, 2015.

[24] S.V. Glass, B. Yeh, B.J. Herzog, Effects of exterior insulation on moisture performance of wood-frame walls in the Pacific Northwest: measurements and hygrothermal modeling, in: Proceedings of the 3rd Residential Building Design & Construction Conference, University Park, PA, USA, March 2-3, 2016, pp. 292–311.

[25] E. Vereecken, S. Roels, Review of mould prediction models and their influence on mould risk evaluation, Build. Environ. 51 (2012) 296–310.

[26] S. Thelandersson, T. Isaksson, Mould resistance design (MRD) model for evaluation of risk for microbial growth under varying climate conditions, Build. Environ. 65 (2013) 18–25.

[27] K. Pietrzyk, A systemic approach to moisture problems in buildings for mould safety modelling, Build. Environ. 86 (2015) 50–60.

[28] H. Viitanen, J. Vinha, K. Salminen, T. Ojanen, R. Peuhkuri, L. Paajanen, et al., Moisture and bio-deterioration risk of building materials and structures, J. Build. Phys. 33 (2010) 201–224.

[29] H. Viitanen, T. Toratti, L. Makkonen, R. Peuhkuri, T. Ojanen, L. Ruokolainen, et al., Towards modelling of decay risk of wooden materials, Eur. J. Wood Wood Prod. 68 (2010) 303–313.

[30] H. Saito, K. Fukuda, T. Sawachi, Integration model of hygrothermal analysis

with decay process for durability assessment of building envelopes, Build. Simul. 5 (2012) 315–324.
[31] T. Isaksson, C. Brischke, S. Thelandersson, Development of decay performance models for outdoor timber structures, Mater. Struct. 46 (2013) 1209–1225.
[32] C. Brischke, L. Meyer-Veltrup, Modelling timber decay caused by brown rot fungi, Mater. Struct. 49 (2016) 3281–3291.
[33] S.L. Zelinka, D. Derome, S.V. Glass, Combining hygrothermal and corrosion models to predict corrosion of metal fasteners embedded in wood, Build. Environ. 46 (2011) 2060–2068.
[34] S.L. Zelinka, S.V. Glass, D. Derome, The effect of moisture content on the corrosion of fasteners embedded in wood subjected to alkaline copper quaternary treatment, Corros. Sci. 83 (2014) 67–74.
[35] S.L. Zelinka, S.V. Glass, C.R. Boardman, D. Derome, Comparison of the corrosion of fasteners embedded in wood measured in outdoor exposure with the predictions from a combined hygrothermal-corrosion model, Corros. Sci. 102 (2016) 178–185.
[36] P.I. Morris, Understanding Biodeterioration of Wood in Structures, Forinteck Canada Corp., British Columbia Building Envelope Council. http://cwc.ca/wp-content/uploads/aboutdecay-biodeterioration.pdf (Accessed 15 November 2016).
[37] C.A. Clausen, Wood Handbook, Ch. 14: Biodeterioration of Wood, Forest Products Laboratory, Madison, WI, 2010. FPL-GTR-190, http://www.fpl.fs.fed.us/documnts/fplgtr/fplgtr190/chapter_14.pdf (Accessed 15 November 2016).
[38] C.G. Carll, T.L. Highley, Decay of wood and wood-based products above ground in buildings, J. Test. Eval. 27 (2) (1999) 150–158.
[39] L. Arena, P. Mantha, Moisture Research – Optimizing Wall Assemblies, US DOE, Building Technologies Program, 2013, http://dx.doi.org/10.2172/1079731. Report DOE/GO-102013–3813.
[40] S.M. Cornick, W. Maref, F. Tariku, Verification and Validation: Establishing Confidence in Hygrothermal Tools, National Research Council of Canada, 2009. Research Report IRC-RR-278.
[41] A. Karagiozis, Application of advanced tools to develop energy efficient building envelopes that are durable, in: Proceedings, Performance of Exterior Envelopes of Whole Buildings IX International Conference, Clearwater Beach, FL, USA, 5–10 December 2004.
[42] G. Finch, J. Straube, Ventilated wall claddings: review, field performance, and hygrothermal modeling, in: Proceedings, Thermal Performance of the Exterior Envelopes of Whole Buildings X International Conference, Clearwater Beach, FL, USA, 2–7 December 2007.
[43] F. Tariku, S.M. Cornick, M.A. Lacasse, Simulation of wind-driven rain penetration effects on the performance of a stucco-clad wall, in: Proceedings, Thermal Performance of the Exterior Envelopes of Whole Buildings X International Conference, Clearwater Beach, FL, USA, 2007.
[44] J. Straube, J. Smegal, Building America Special Research Project: High-r Walls Case Study Analysis, Research Report BA-0903, Building Science Corporation, Somerville, MA, USA, 2009.
[45] M. Pazera, M. Salonvaara, Drying characteristics of spray-applied cellulose fiber insulation, J. Test. Eval. 39 (2011) 219–229.
[46] S. Pallin, M. Kehrer, W.A. Miller, A hygrothermal risk analysis applied to residential unvented attics, in: Proceedings, Thermal Performance of the Exterior Envelopes of Whole Buildings XII International Conference, Clearwater Beach, FL, USA, 1–5 December 2013.
[47] M. Salonvaara, A. Karagiozis, A. Desjarlais, Moisture performance of sealed attics in climate zones 1 to 4, in: Proceedings, Thermal Performance of the Exterior Envelopes of Whole Buildings XII International Conference, Clearwater Beach, FL, USA, 1–5 December 2013.
[48] H.H. Saber, W. Maref, Risk of condensation and mould growth in wood-frame wall systems with different exterior insulations, in: Proceedings of Building Enclosure Science & Technology Conf. (BEST4), April 12-15, 2015 (Kansas City, Missouri, USA).
[49] S.V. Glass, A. TenWolde, Review of In-service Moisture and Temperature Conditions in Wood-frame Buildings, Forest Products Laboratory, Madison, WI, 2007. FPL-GTR-174.
[50] J. Langmans, R. Klein, S. Roels, Hygrothermal risks of using exterior air barrier systems for highly insulated light weight walls: a laboratory investigation, Build. Environ. 56 (2012) 192–202.
[51] D.M. Onysko, C. Schumacher, P. Garrahan, Field measurements of moisture in building materials and assemblies: pitfalls and error assessment, in: Proceedings of BEST 1 Conference, June 10-12, 2008 (Minneapolis, MN).
[52] J. Straube, D. Onysko, C. Schumacher, Methodology and design of field experiments for monitoring hygrothermal performance of wood frame enclosures, J. Therm. Env. Buid. Sci. 26 (2) (2002) 123–151, http://dx.doi.org/10.1106/109719602028098.
[53] W.L. James, Electric Moisture Meters for Wood, Forest Products Laboratory, Madison, WI., 1963. FPL-08.
[54] W.L. James, Electric Moisture Meters for Wood, Forest Products Laboratory, Madison, WI., 1988. FPL-GTR-6.
[55] F. Pfaff, P. Garrahan, New temperature correction factors for the portable resistance-type moisture meter, For. Prod. J. 36 (3) (1986) 28–30.
[56] P. Garrahan, Moisture meter correction factors, in: Proceeds of a Seminar on In-Grade Testing of Structural Lumber, Madison, WI,, Forest Products Laboratory, US Forest Service, Madison WI, April 25-26, 1988.
[57] W. James, Effect of temperature on readings of electric moisture meters, For. Prod. J. 18 (10) (1968) 23–31.
[58] C.R. Boardman, S.V. Glass, C.G. Carll, Moisture meter calibrations for untreated and ACQ-treated southern yellow pine lumber and plywood, J. Test. Eval. 40 (1) (2012) JTE103895.
[59] W. Maref, M.A. Lacasse, D. Booth, Experimental assessment of hygrothermal properties of wood-frame wall assemblies – moisture content calibration curve for OSB using moisture pins, J. ASTM Int. 7 (1) (2010), http://dx.doi.org/10.1520/JAI102091.
[60] S. Zelinka, S.V. Glass, D.S. Stone, A percolation model for electrical conduction in wood with implications for wood-water relations, Wood Fiber Sci. 40 (4) (2008) 544–552.
[61] R.E. Hummel, Electrical Properties of Polymers, Ceramics, Dielectrics, and Amorphous Materials, Ch. 9 in Electronic Properties of Materials, Springer-Verlag, 2001.
[62] S. Aziz, Z.G.Z. Abidin, Electrical conduction mechanism in solid polymer electrolytes: new concepts to Arrhenius equation, J. Soft Matter (2013), http://dx.doi.org/10.1155/2013/323868.
[63] S.D. Kasap, Principles of Electronic Materials and Devices (Chapter 2). Electrical and Thermal Conduction in Solids, third ed., McGraw-Hill, 2015.
[64] ASTM D4442. Standard Test Methods for Direct Moisture Content Measurement of Wood and Wood-Based Materials, American Standard for Testing and Materials, West Conshohocken, PA, 2015.
[65] SAS. Cary, NC: SAS Institute, Inc., 2013. http://support.sas.com/documentation/94/. (November 16, 2016).
[66] R Core Team, R: A Language and Environment for Statistical Computing. R Foundation for Statistical Computing, 2016. Vienna, Austria, https://www.R-project.org/.
[67] S.C. Zylkowski, Dimensional Stability of Structural-Use Panels, Report No. R&D86L-43, American Plywood Association, Tacoma, WA, 1986.
[68] R.F. Richards, D.M. Burch, W.C. Thomas, Water vapor sorption measurements of common building materials, ASHRAE Trans. 98 (1992) 475–483.
[69] N. Sekino, A. Suematsu, H. Kohrai, E. Yasui, Measurements of sorption isotherms of selected commercial wood-based panels and predictions of moisture content changes in service, Mokuzai Gakkaishi 45 (1999) 237–243.
[70] Q.L. Wu, Y.K. Ren, Characterization of sorption behavior of oriented strandboard under long-term cyclic humidity exposure condition, Wood Fiber Sci. 32 (2000) 404–418.
[71] M.K. Kumaran, J.C. Lackey, N. Normandin, F. Tariku, D. van Reenen, A Thermal and Moisture Transport Property Database for Common Building and Insulating Materials: Final Report from ASHRAE Research Project 1018-RP, American Society of Heating, Refrigerating and Air-Conditioning Engineers, Inc., Atlanta, GA, 2002.
[72] M.K. Kumaran, J.C. Lackey, N. Normandin, F. Tariku, D. Van Reenen, Variations in the hygrothermal properties of several wood-based building products, in: J. Carmeliet, H. Hens, G. Vermeir (Eds.), Research in Building Physics: Proceedings of the 2nd International Conference on Building Physics, Swets & Zeitlinger B.V., Antwerpen, Belgium, 2003, pp. 35–42.
[73] A. Karagiozis, K. Wilkes, Hygrothermal Properties of Selected Materials. Report 2, ASHRAE Research Project 1091, Development of Design Strategies for Rainscreen and Sheathing Membrane Performance in Wood Frame Walls, American Society of Heating, Refrigerating and Air-Conditioning Engineers, Inc., Atlanta, GA, USA, 2004.
[74] T. Ojanen, J. Ahonen, C.J. Simonson, Moisture performance characteristics of OSB and spruce plywood exterior sheathing products, in: P. Fazio, H. Ge, J. Rao, G. Desmarais (Eds.), Research in Building Physics and Building Engineering: Proceedings of the Third International Building Physics Conference, Taylor & Francis, Montreal, Canada, 2006, pp. 97–105.
[75] I.D. Hartley, S.Q. Wang, Y. Zhang, Water vapor sorption isotherm modeling of commercial oriented strand panel based on species groups and resin type, Build. Environ. 42 (2007) 3655–3659.